Discrimination of Quarry Blasts from Micro Earthquakes in the Surendranagar region of Saurashtra Horst, Northwestern India

Mayank Dixit (caimera2007@gmail.com)
Institute of Seismological Research
Ketan Singh Roy
Institute of Seismological Research
Arpan Shastri
Institute of Seismological Research

Full paper

Keywords: P/S waves ratio, Coda decay rate, Spectrogram Analysis, Surendranagar

Posted Date: August 4th, 2020

DOI: https://doi.org/10.21203/rs.3.rs-50708/v1

Abstract

The complex and covert phenomenon undergoing in the earth's interior is revealed by the seismic waves propagating to the surface. The main objective of this study is to uphold the difference in the nature of waves transmitted due to quarry blasts and earthquakes and differentiate the tremors caused by the two. A total of ~1300 ground motions recorded at different broadband seismic stations of Saurashtra, Gujarat, observed from 2012 to 2016 of magnitude greater than or equal to 1.4 were considered for the study. These recordings have been obtained from the seismic network established and maintained by Seismic Data Analysis Center (SeiDAC), Institute of Seismological Research (ISR), Gandhinagar, Gujarat. In this investigation, ground motions of frequency greater than 1Hz were considered and statistical method (maximum of P to S (P/S) waves amplitude ratio) was applied for four mutually exclusive frequency bands such as 2 to 4, 4 to 6, 6 to 8, 8 to 10 and a common bin from 1 to 10 Hz. The outcome of this investigation suggested that ~10% of the examined ground motion records were caused due to quarry blasts and the rest as a consequence of earthquakes. Application of the coda decay rate method revealed that the coda decay rate Qc^{1} is significantly higher for quarry blasts than earthquakes of lower frequencies (1.5 and 3.0 Hz). The spectrogram analysis affirms the distinction between quarry blasts and earthquakes in terms of varying frequency content. The detailed investigation brought forward an intriguing remark about mining-induced seismicity as more seismic activity was observed during the daytime when compared with the after-dark recordings. The findings of this investigation may contribute to the existing knowledge base on earthquakes in addition to creating a distinction between the natural and manmade earthquakes.

1.0 Introduction

Recognition of quarry blasts in a seismic data set is an arduous task. Many seismic organization endeavors to identify and mark quarry blasts during their routine data analysis. A careful analysis of waveforms and their spectra can often find telltale signs of explosion characteristics (*Hedlinet al., 1990; Su et al., 1991; Wuster, 1993; Musil and Plesinger, 1996*), but such detailed analysis is impractical when dealing with large volumes of data on a daily basis or when re-examining existing seismicity datasets (*Wiemer and Baer 2000*). Numerous studies of discrimination methods both in time and frequency domain are in vogue. These methods can be generally divided into (I) amplitude ratio between seismic phases, like Pn/Sn and Pn/Lg (e.g., *Baumgardt and Young, 1990*), Lg/Pg and Lg/ Rg(e.g., *Wüster1993*), (II) Spectral methods (e.g., *Taylor et al., 1998; Hedlin, 1998*), (III) time and frequency domains (*Sertçelik and Başer, 2010; Öğütçü et al. 2011; Kartal and Horasan, 2011*), (IV) Coda wave studies (*e.g., Su et al., 1991; Hartse et al., 1995*).

In many areas, quarries are well established and produce frequent explosions that can be recognized by their locations. Quarry blasts commonly occur during the working hours (8 a.m. and 5 p.m. local time) of the day (*Horasan et al. 2009; Wiemer and Baer 2000; Yilmaz et al. 2012*). Earthquakes, on the other hand, can occur at any hour during the day and night. The energy source for an earthquake is tectonic strain accumulated by the relative motion of the two blocks and has wider bandwidth, while in a quarry blast all of the energy is suddenly (within milliseconds) released in the form of heat. In the case of earthquakes, the energy of the S wave is greater than that of the P wave, while in case of quarry blast P wave energy is larger. Both these sources generate seismic waves but the nature of observed seismograms is quite different. Usually strong secondary waves are observed in earthquakes but such phases are absent in quarry blast. Additionally, quarry blasts occur on land and near the surface. In another case, commonly quarry blasts have magnitudes and focal depths smaller than about 3.0 and 10 Km respectively (*Yilmaz et al. 2012*).

In Northwestern Deccan Volcanic Province of peninsula India, the intraplate Gujarat region is divided into three regions, i.e., Kachchh rift basin, Mainland and Saurashtra horst (*Biswas, 1982; 1987*) (Figure 1a). Before the year 2001, the study and understanding regarding the fault system in the region were inadequate for a comprehensive knowledge of geodynamic mechanisms. However, on January 26, 2001, the devastating Mw7.7 Bhuj earthquake reawakened attention to the high earthquake risk in the Gujarat region. As a result of the Bhuj earthquake, during 2006, the ISR installed the Gujarat Seismic Network (GSNet) permanently. Currently, 54 accelerographs and 60 three-component high-resolution digital seismographs covering the entire Gujarat region provides an excellent opportunity to decipher the genesis and geodynamic mechanism of earthquakes in the region (*ISR annual report, 2016*).

In this study, we discriminate surface quarry blasts from earthquakes in seismic events between 2012 and 2016 in the Surendranagar region of Saurashtra horst recorded by the (GSNet), ISR, Gandhinagar, Gujarat (Figure 1a). The region has significant minerals wealth such as Fire clay, Silica sand, Black Stone, Sandstone, etc. About 25% of India's salt supply comes from mining in the Surendranagar area (*Department of Mines and Geology, Surendranagar*). A large number of blasts have been detonated in different quarries which are recorded by the GSNet and are used in the present study. However, these ground motion records befoul the seismicity catalogs causing the hazard and seismic risk studies erroneous, so these records should be excluded from the regional catalogs.

By observing preliminary histograms, we identified more events in daytime as compared to the dark events (Figure 1b). Additionally, we also observed a fall in seismicity during the Indian monsoon season (Figure 1c). This motivates us to perform the study to discriminate between quarry blasts and earthquakes.

2.0 Data And Methodology

The ISR has been operating the GSNet of 09 broadband stations in the Saurashtra region (Figure 1a) which is operated and maintained by the SeiDAC since 2006 (*ISR annual report, 2016*). The homogeneity and magnitude of completeness Mc of any catalog are critical for any statistical analysis. We first calculated the magnitude of completeness Mc using software ZMAP *(Wiemer, 2001*) and found equal to 1.4 (Figure S1). After that, we also removed those events which have signal to noise ratio (SNR) lower than of 2.0 (Figure S2). The raw waveform data were corrected by removing the instrument response. The magnitudes, depths and locations of recorded events are calculated by SEISAN software (*Havskov & Ottemoller, 1999*) using 09 stations. These events occurred in SSW direction from the Surendranagar (SUR) station (Figure 1a).

Since quarry blasts generally occurred during the day time hours, the ratio of day to night time events are quantified by computing Qm (Quarry Mining) statistics (*Kekovali et al., 2011*) and defined as:

$$Qm = \frac{logT[2Td - Tn]}{[2Tn + Td]}$$

Where, T is the total number of events, Td, and Tn are the total number of events during day and night time respectively. An indicative value of the day/night time ratio is ≥1.5 (*Wiemer and Baer, 2000*; *Kekovali et al., 2011*).

In the discrimination analysis, the first method used in the study plots the amplitude peak ratio of the P to S waves versus magnitude and epicentral distance in the time domain of seismogram. The quarry blasts (P/S>1) can generate a little S- wave energy and relative P/S wave amplitudes could be used as one technique to distinguish them from earthquakes (P/S<1). For every 1300 seismic events, the P and S wave amplitudes were taken from vertical and horizontal components respectively of the nearest station Surendranagar (SUR).

After the discrimination criteria of the P/S amplitude ratio, to validate our results we used the coda wave method (*Aki and Chouet, 1975; Su et al., 1991*). The decay of the coda wave is independent of the wave path. However, its decay depends on the average properties of the area neighboring the source and receiver (*Su et al., 1991*). This property gives an opportunity to isolate the explosion and earthquake source from path effects and evaluate their source differences. In this method, for both quarry blasts and earthquakes at the same station SUR, we obtained coda decay curves over different frequency bands (1.5 to 12 Hz).

Quarry blasts generally have shorter bandwidth, high frequency, are impulsive in nature (*Yilmaz et al., 2013*). Fundament mode Rayleigh wave (Rg) is generally associated with quarry blasts and very shallow focus earthquakes (*Kafka 1990*). Additionally, the primary phase P is dominant in the quarry blasts and the S phase is generally absent. Whereas, on the other hand, the amplitude of the S wave is greater than the P phase in earthquakes. These phases are difficult to identify in time series. Hence, we calculated the Short-Time Fourier transform which divides the signal into small slices of the same width and performs Fourier analysis on each segment to calculate the frequencies in each slice (*Cohen 1995; Yilmaz et al., 2013).*

3.0 Result And Discussion

In this study, we discriminated the quarry blasts from microearthquakes in the Surendranagar region in Saurashtra provenance of Northwestern India.

3.1 P/S amplitude ratio

The key to the efficacious discrimination of numerous types of seismic sources is the clear observation of the signals released from seismic sources (*Kim et al. 1998*). One of the most important problems is the correction of the effects of the source to receiver paths in the observed regional signals (*Kim and Richards 1996*). After removing the free-surface effects from our data, we calculated the P/S ratio for four mutually exclusive frequency bands: 2 to 4, 4 to 6, 6 to 8, 8 to 10, and a common bin from 1 to 10 Hz. The ratio of P/S is calculated at the nearest station SUR and plotted against the epicenter and magnitude of the events. Figure 2 and 3 shows the P/S ratios over five frequency bands. In this figure, it appeared that the best separation is observed in the 8 to 10 Hz range. Since S wave amplitude of the earthquakes is greater than P wave and, P wave is dominant in quarry blasts, hence P/S>1 are quarry blasts and P/S<1 are earthquakes. Kim et al. (1998) found that the best separation between quarry blasts and earthquakes was in 6-8 Hz. We observed that the identified quarry blasts are in the range between 22 and 38 km (Figure 2), additionally, the observed quarry blasts are between the magnitude range of 1.4 and 2.2 (Figure 3).

3.2 Short-Time Fourier transform

After the P/S discrimination, many events are close to the separation line (Figure 2 and 3). If the P/S ratio is close to one, then it indicates that the amplitude of P and S waves is somewhere equal. In these cases, we used Short-time Fourier transform to decide whether these events are earthquakes or quarry blasts. This method is a valuable tool to study the frequency and amplitude content of the entire seismic waveforms (*Kim et al. 1994*). In quarry blasts, the energy released in a quick time and maximum amplitude occurred at the starting time of the record (*Yilmaz et al. 2012).* For earthquakes, P wave amplitude is much shorter than S wave and maximum energy observed after the P wave train. The figure 4 and 5 shows the spectrogram of quarry blast and earthquake respectively. From figure 4, we observed that the P wave is dominated in the seismogram. P wave energy is shown in green color and we found no other phase in the spectrogram. Figure 5 shows that the amplitude of the S wave is much larger than those of P wave and represented in red and green color respectively. Considering the above criteria related to maximum released energy, which confirms that the event in figure 4 is quarry blast and figure 5 shows an earthquake.

Additionally, we found Rg phases in both quarry blast and earthquake at lower frequencies (0.5-2.5 Hz). Similar features have been observed by Yilmaz et al. (2012). This indicates that the above events are at a very shallow depth.

3.3 Coda Wave method

The coda Qc has been computed using the single backscattering model proposed by Aki and Chouet (1975). This model clarifies that coda waves are backscattered body waves generated by randomly distributed heterogeneity in the Earth's crust and upper mantle. Each wavelet is scattered only once before reaching the receiver. Data from both quarry blast and earthquakes sources were processed by an identical procedure to study the possible differences in coda attenuation. Figure 6a, c, g, e shows the measured Qc of earthquakes as a function of lapse time for frequencies 1.5, 3.0, 6.0 and 12 Hz, respectively, while Figure 3b, d, f, h shows the corresponding results for quarry blasts. The resultants Qc^{-1} values for all earthquakes were plotted together. The solid line connects the mean points calculated by averaging the individual measurements. By comparing these figures, we found that for the frequencies of 1.5 and 3.0 Hz, Qc^{-1} shows significant differences between quarry blasts and earthquakes. The Qc^{-1} values at these low frequencies are greater for quarry blasts than for earthquakes at lower frequencies of 1.5 and 3.0 Hz. It is elucidated that in contrast to earthquakes, more surface waves are generated in blasts as they originate from extremely shallow depths. Because the propagation paths of surface waves being confined at superficial depths thus the surface waves attenuate quickly. At t>20 sec for 6 and 12 Hz and at t > 30 sec for 1.5 and 3.0 Hz, body waves become dominant over surface waves resulting in same coda decay rate and path effects for both blasts and earthquakes which further indicates that delayed lapse time is dominated almost certainly by S waves, i.e a single type of body wave, excluding coda waves at lower frequencies which are associated with the surface wave (*Su et al., 1991*).

3.4 Induced Seismicity

The Qc value of 2.75 (Figure 7c) observed after the discrimination is greater than the threshold value of 1.5. This suggests that the observed earthquake activity is more during the daytime when compared with the after-dark recordings (Figure 7), which indicates that these observed micro-earthquakes may be mining-induced.

Mining induced seismicity is a well-known long studied phenomenon throughout the world (e.g. *Gibowicz, 1990; Johnston, 1992)*. The decrease in normal stress or an increase in the shear stress acting on a fault is responsible for the mining-induced seismicity (*McGarr et al., 1999*). In this study, we found numerous microearthquakes following the quarry blasts (Figure 8). However, we do not identify these microearthquakes instantaneously/during or just after the passage of the quarry blasts waves i.e. these microearthquakes are observed with some delays. This observation may suggest that the dynamic stress imposed by the quarry blasts may have invoked the faults in the study area. For instance, when a fault (or population of faults) is near to failure, then it is more susceptible to dynamic stress perturbation. In other words, the addition of any small stress perturbation on a critically stressed fault can lead to the occurrence of brittle failure (*Brodsky & van der Elst, 2014; Gomberg et al., 1998*). The subcritical crack growth model substantiates the aforementioned and puts forward the idea of earthquake nucleation (*Atkinson, 1984*), which suggests that the intensity of stress at the crack tip (relative to crack size) governs the rate of crack growth. At the initial stage, the crack extends very slowly and then grows rapidly with the unexpected rise of/increase in stresses at the crack tip eventually leading to what is called apparently delayed fault rupture (*Atkinson, 1984; Rinne, 2008*). However, we cannot completely rule out the involvement of earthquakes that are occurred by natural stress perturbations in the study area (Figure 7c).

3.5 Seasonal and Diurnal observations

India is a land of festivals and Indians give special importance to them. Some of the main festivals which are celebrated include Diwali, Holi, Raksha Bandhan, and Pongal. Indians also hold great regard for National festivals like Independence (15^{th} August) and Republic Day (26^{th} January). We examined the ISR seismic catalog four days before and after these festivals. We found no signals of quarry blasts during these festival days (Figure 9), as quarry blasts are operated only during the working days. Additionally, on the other hand, we also inspected the ISR catalog during the days of the week (Sunday to Saturday). We found the events on weekends also (Figure 7e, f). Hence, we cannot completely rule out the operations of illegal quarry blasts and mining during the holidays (*The Indian Express, January 01, 2020; The Telegraph, January 06, 2020*). Illegal mining is a perennial problem in India (*India TV news, June 18, 2018*), however, to operate the mining during the monsoon is extremely difficult. We observed that during the Indian monsoon (June-September) the seismicity decreases and it increases steadily after the monsoon because during the monsoon season the quarries are not operational.

4.0 Conclusion

We analyzed seismic events recorded between 2012 and 2016 to discriminate quarry blasts from earthquakes in the Surendranagar region of Northwestern India. We applied the P/S amplitude ratio, Coda decay rate and Short-time Fourier transform to decide whether the recorded events are earthquakes or quarry blasts. After applying the discrimination methods, we identified 120 quarry blasts and ~1100 microearthquakes (induced+natural). This suggested that 10% of the examined ground motion records are due to quarry blasts and the rest as a consequence of earthquakes. The identified quarry blasts are occurred in the day time and concentrated in one place only (Figure 10). Additionally, most of the induced microearthquakes are identified near the quarry blast region (Figure 10). The largest identified quarry blast during the studied period is of magnitude 2.2. We also identified many machinery used near the quarry blast operations (Figure S3).

List Of Abbreviations

SeiDAC: Seismic Data Analysis Center

ISR: Institute of Seismological Research

P/S: P and S wave amplitude

GSNet: Gujarat Seismic Network

SNR: Signal to noise ratio

SUR: Surendranagar

Qm: Quarry mining

Declarations

Availability of data and materials

The datasets analyzed during the current study are not publicly available because it is of an ongoing project, but may be available by the permission of the Director-General, ISR on reasonable request.

Competing interests

Not applicable

Funding

ISR provided the financial support for carrying out this study

Authors' contributions

MD analyzed and interpreted the data and was a major contributor in writing the manuscript. KSR made shell script. AS calculated the Qc inverse values. All authors read and approved the final manuscript.

Acknowledgments

We sincerely thank Dr. M. Ravi Kumar, the Director-General, ISR, for all supports and encouragement for carrying this research and for the permission to publish the work. We are thankful to ISR for providing financial support for carrying out this study. We are also thankful to Dr. Santosh Kumar and his team for providing us the valuable data. MD is thankful to Dr. S. Sekhar for useful discussions during the study.

References

1. Aki, K., & Chouet (1975). Origin of coda waves: source, attenuation and scattering effects, Journal of Geophysical Research. 80, 3322-3342.

2. Atkinson, B. K. (1984). Subcritical crack growth in geological materials. *Journal of Geophysical Research*, *89*(B6), 4077–4114. https://doi. org/10.1029/JB089iB06p04077
3. Baumgardt, D.R., &Young, G.B. (1990). Regional seismic waveform discriminates and case-based event identification using regional arrays. Bull Seism Soc Am 80:1874–1892.
4. Brodsky, E. E., & van der Elst, N. J. (2014). The uses of dynamic earthquake triggering. *Annual Review of Earth and Planetary Sciences*, *42*(1), 317–339. https://doi.org/10.1146/annurev-earth-060313-054648
5. Exclusive: “Jungle raj” of send mafia rampant in many states; MLA, police force in line of fire, June 18, 2018, India Tv news (https://www.indiatvnews.com/news/india-exclusive-jungle-raj-of-sand-mafia-rampant-in-many-states-mlas-police-force-in-line-of-fire-448701)
6. Ge, Z., &Xie, X. (2003). Rg-Lg coupling as aLg-wave exciation mechanism, AGU fall meeting.
7. Gibowicz, S. J., Harjes, H.-R, and Schafer, M. (1990). Source parameters of seismic events at Heinrich Robert mine, Ruhr basin, Federal Republic of Germany: Evidence for nondouble-couple events.*Bull. Seismol. Soc. Am.* 80, 88-109
8. Gitterman, Y., &Shapira, A. (1993) Spectral discrimination of underwater explosions. Isr J Earth Sci 42:37–44.
9. Gomberg, J., Beeler, N. M., Blanpied, M. L., & Bodin, P. (1998). Earthquake triggering by transient and static deformations. *Journal of Geophysical Research*, *103*(B10), 24,411–24,426. https://doi.org/10.1029/98JB01125
10. FIRs filed in 2.16% of 38,100 cases of illegal mining in Gujarat, January 01, 2020, The Indian Express (https://indianexpress.com/article/cities/ahmedabad/firs-filed-in-2-16-of-38100-cases-of-illegal-mining-in-state-6194379/)
11. Havskov, J., &Ottemoller, L. (1999). SeisAn earthquake analysis software. Seismological Research Letters, 70(5), 532–534. https://doi.org/10.1785/gssrl.70.5.532 I
12. Hedlin, M., Minster, J., &Orcutt, J. (1990). An automatic means to discriminate between earthquakes and quarry blasts, *Bull. Seism. Soc.Am.* **80**, 2143–2160.
13. Hedlin, M. A. (1998). A global test of a time-frequency small-event discriminant, Bull. Seismol. Soc. Am. 88, 973–988
14. Horasan, G., Boztepe-Güney, A., Küsmezer, A., Bekler, F., Öğütçü, Z., Musaoğlu, N., (2009). Contamination of seismicity catalogs by quarry blasts: an example from Istanbul and its vicinity, northwestern Turkey. J Asian Earth Sci 34:90–99.
15. Johnston, J. C. (1992). Rockbursts from a global perspective. In "Induced Seismicity" (P. Knoll, ed.). Balkema, Rotterdam, pp. 63-78.
16. Kafka A,L (1990) Rg as a depth discriminant for earthquakes and explosions: a case study in new england, Bulletin of the Seismological Society of America, Vol. 80, No. 2, pp. 373 394
17. Kartal, Ö.F., &Horasan, G., (2011). Trabzon vecivarındakidepremvepatlatmaverilerininbirbirindenayırtedilmesi (Discrimination of quarry blasts

and earthquakes in Trabzon and its vicinity). SAÜ Fen BilimleriDergisi 15:68–74

18. Kim, Y.Y., Simpson, D.W. & Richards, P.G., 1994. High-frequency spectra of regional phases from earthquakes and chemical explosion, Bull. Seism. Soc. Am., 84, 1365-1386.
19. Kim, W.Y. & Richards, P.G., 1996. Discrimination of regional earthquakes and explosion using three-component, high-frequency digital data, Modern Seismology-Proc. Korea-China Int. Joint Seminar & seism. Workshop, pp. 46-61, Kim, S.G., Seoul, Korea.
20. McGarr A. (1999). On relating apparent stress to the stress causing earthquake fault slip. J. Geophys. Res. 104, 3003-3011.
21. Musil, M., &Plesinger, A. (1996). Discrimination between local microearthquakes and quarry blasts by multilayer perceptrons and Kohonenmaps, *Bull. Seism. Soc. Am.* **86**, 1077–1090.
22. Öğütçü, Z., Horasan, G., &Kalafat, D. (2011). Investigation of micro seismic activity sources in Konya and its vicinity, Central Turkey. Nat Hazards 58:497–509
23. Rinne, M. (2008). *Fracture mechanics and subcritical crack growth approach to model time-dependent failure in brittle rock*. Helsinki: Helsinki University of Technology.
24. Sertçelik, F.,&Başer, O. (2010).GüneyEgeBölgesi'ndeyapayvedoğalkaynaklıtitreşimlerinayırtedilmesi (Discrimination of artificial and natural sourced vibrations in the southern Aegean Region). Yerbilimleri 31:233–245.
25. Su, F., Aki, K.,& Biswas, N. (1991). Discriminating quarry blasts from earthquakes using coda waves, *Bull. Seism. Soc. Am.* **81**, 162–178.
26. Taylor, S. R., N. W. Sherman, and M. D. Denny (1988). Spectral discrimination between NTS explosions and western United States earthquakes at regional distances, Bull. Seismol. Soc. Am. 78, no. 4, 1563–1579.
27. Two killed in stone quarry blast, January 06, 2020, The Telegraph (https://www.telegraphindia.com/jharkhand/2-killed-in-stone-quarry-blast-at-korigrah-in-dumka-district/cid/1733550)
28. Wessel, P., & Smith, W. (1995). New version of the Generic Mapping tools (GMT) version 3.0 released, Eos Trans. AGU 76, 329.
29. Wiemer, S., &Baer, M. (2000). Mapping and removing quarry blast events from seismicity catalogs, short notes. Bull Seism Soc Am 90:525–530
30. Wiemer, S. (2001), A software package to analyze seismicity: ZMAP, Seismol. Res. Lett., 72(3), 373–382, doi:10.1785/gssrl.72.3.373.
31. Wüster, J. (1993). Discrimination of chemical explosions and earthquakes in central Europa—a case study. Bull Seism Soc Am 83:184–1212
32. Yılmaz, S., & Bayrak, Y.,&Çınar, H. (2012). Discrimination of earthquakes and quarry blasts in the eastern Black Sea region of Turkey. J Seismol (2013) 17:721–734

Figures

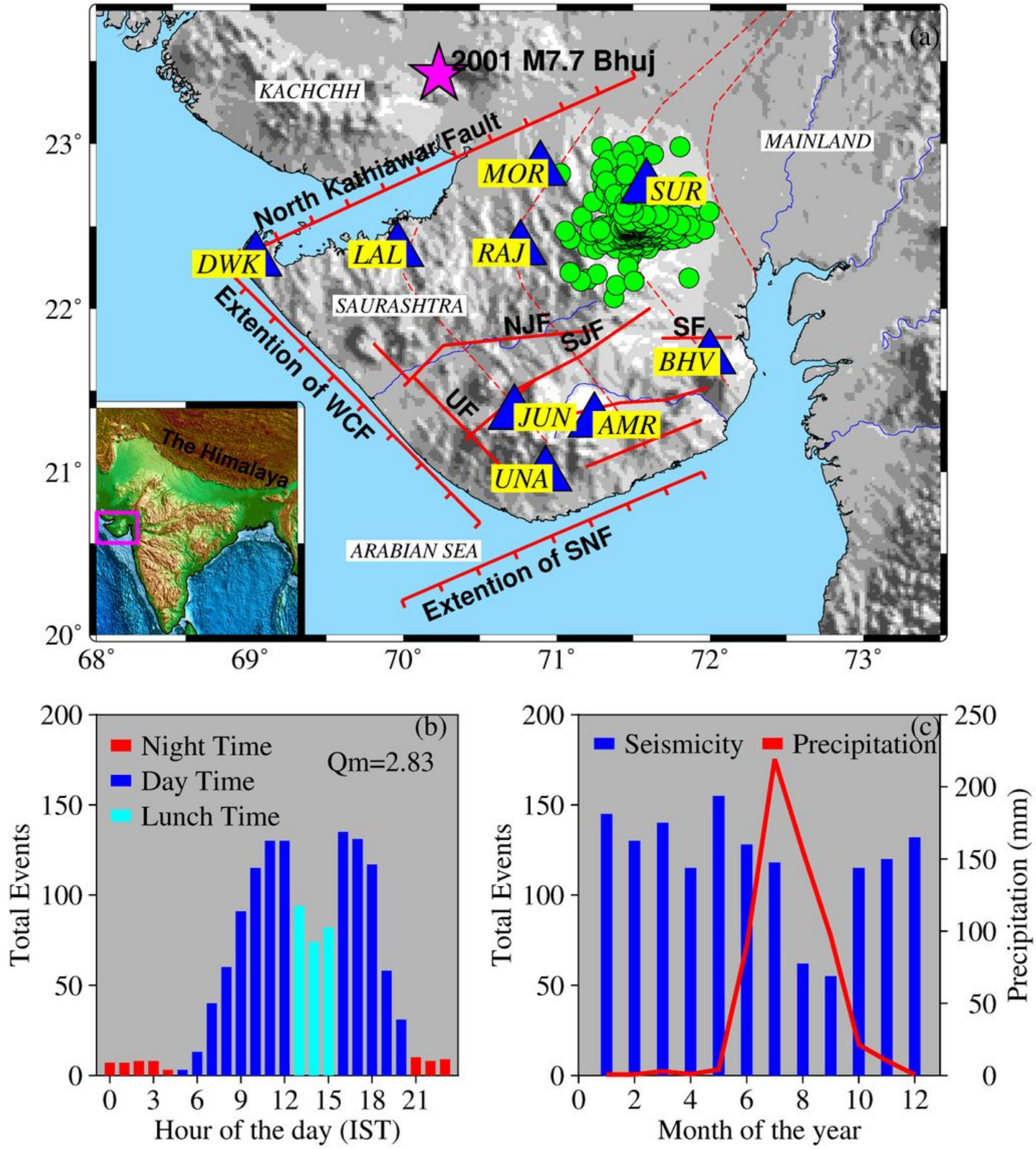

Figure 1

(a) Seismotectonic map view of the Saurashtra horst in Northwestern India. The blue triangles are broad-band stations and red lines are active faults, UF: Umrethi Fault, SF: Saverkindala Fault, SJF: South Junagadh Fault, NJF: North Junagadh Fault, WCF: West coast Fault, SNF: Son-Narmada Fault along with the recorded events between 2012 and 2016 (green circles). The dotted red lines indicate Precambrian trends. The location of Saurashtra in India is shown in bottom left inset map (magenta box). (b)

Distribution of the seismic events by time of day in the study area. The Qm>1.5 indicates that the recorded events are occurred more in day time as compared to dark-recordings which may be an indication of quarry blasts. (c) Histogram of the seismic events by month of year. The seismicity decreases during the monsoon season (July-September), as quarries are not operated in rainy season.

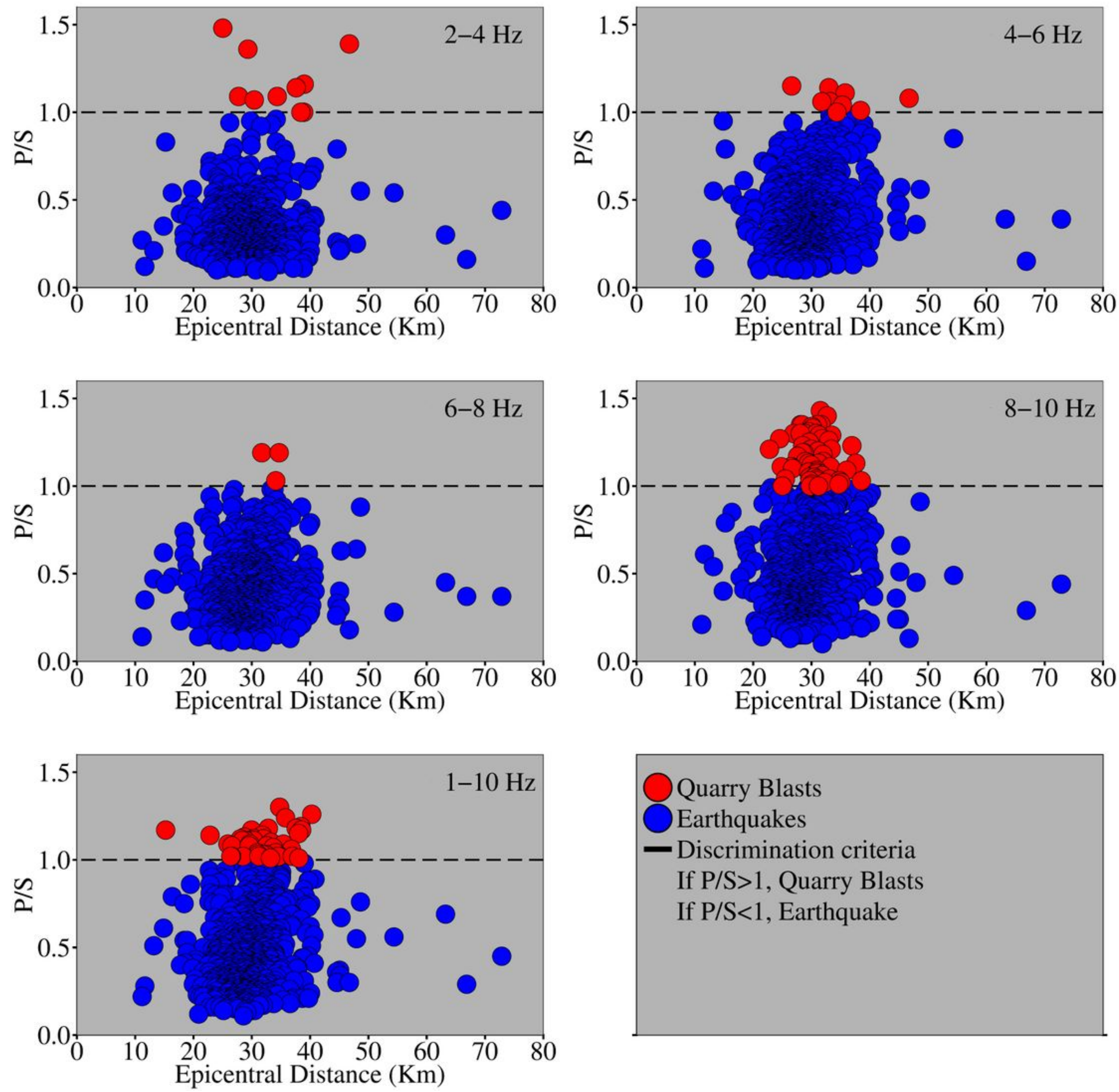

Figure 2

Graphics of P/S ratio versus Epicenter distance for four mutually exclusive frequency bands: 2 to 4, 4 to 6, 6 to 8, 8 to 10 and a common bin from 1 to 10 Hz of recorded events between 2012 and 2016 at station SUR.

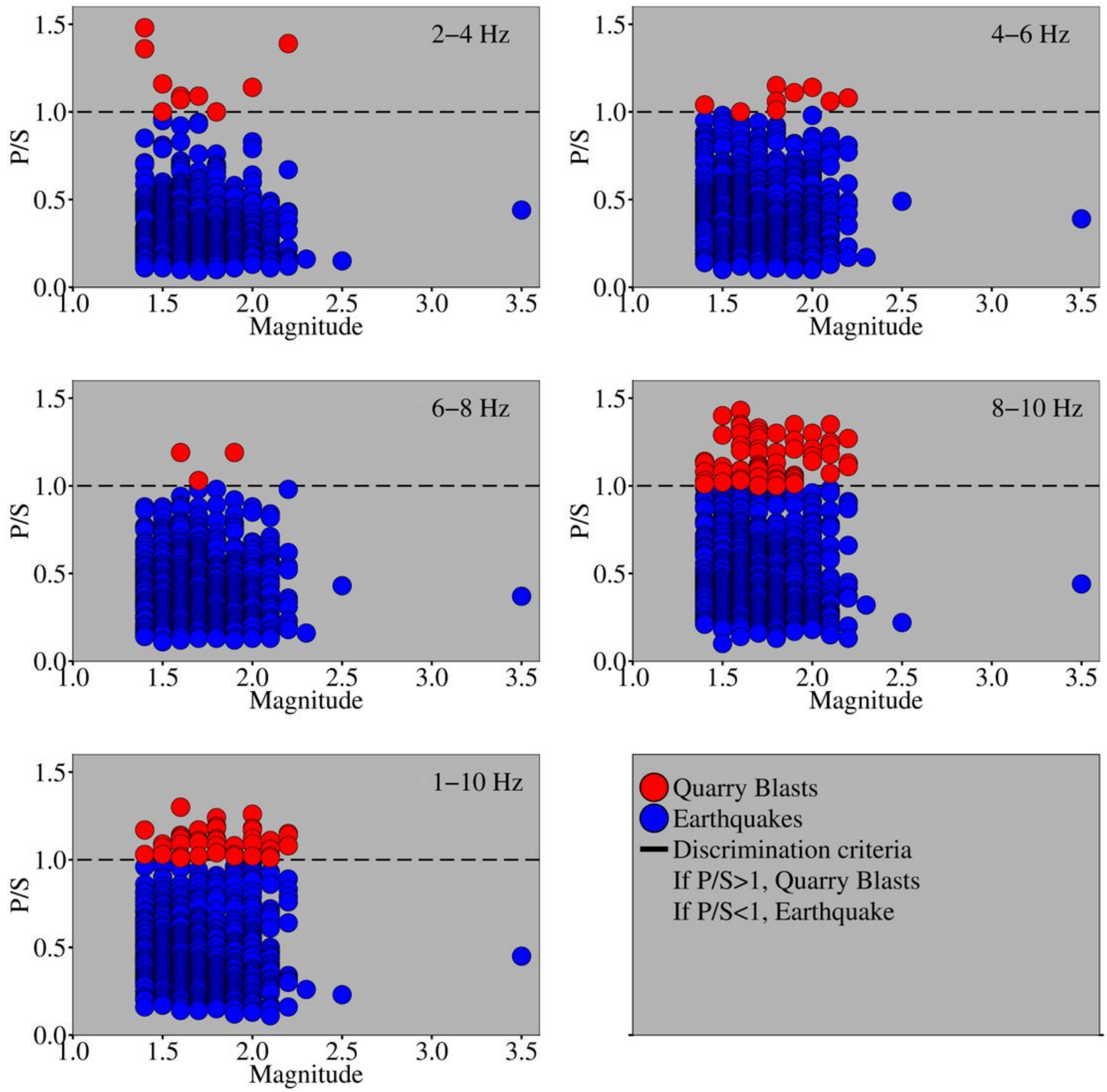

Figure 3

Same as Figure 2 but versus magnitude of the events.

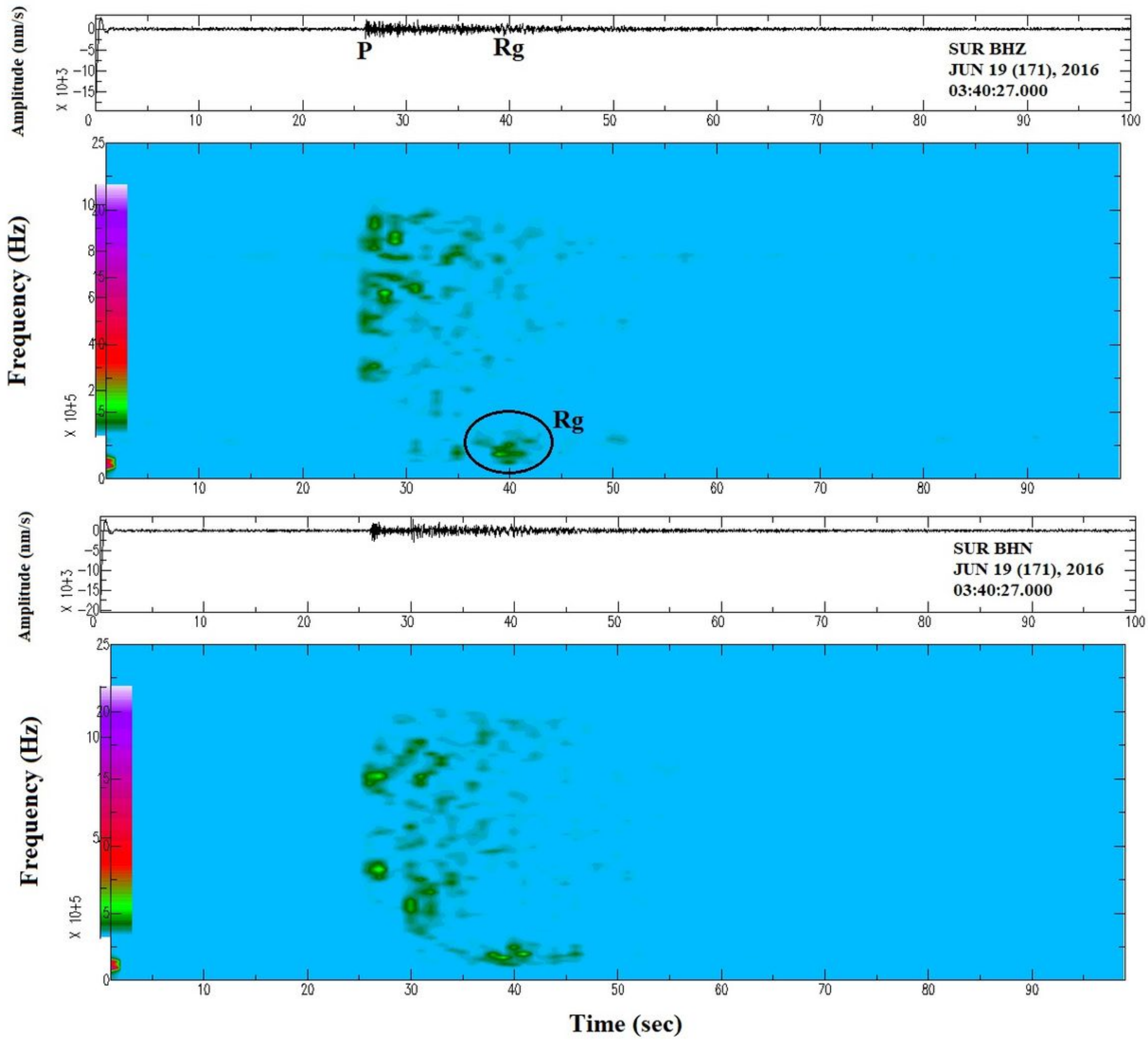

Figure 4

Spectrogram of vertical (Z) and horizontal (N) component of quarry blast recorded at SUR station on June 19, 2016. Rg phase can be observed around at 2.5 Hz.

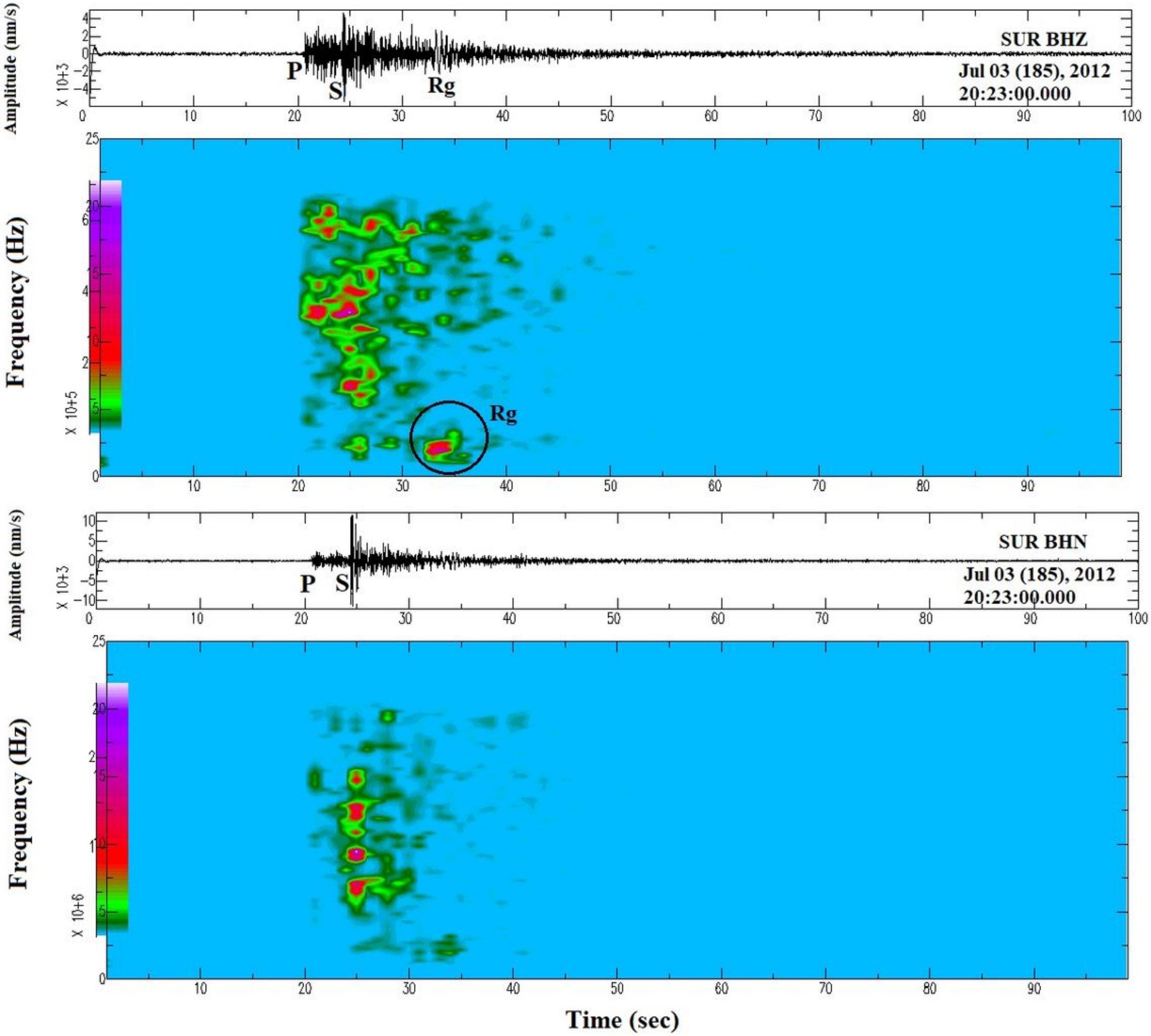

Figure 5

Same as Figure 4 but for earthquake on July 03, 2012. Strong Rg phase can be seen around at 2.5 Hz on the vertical component.

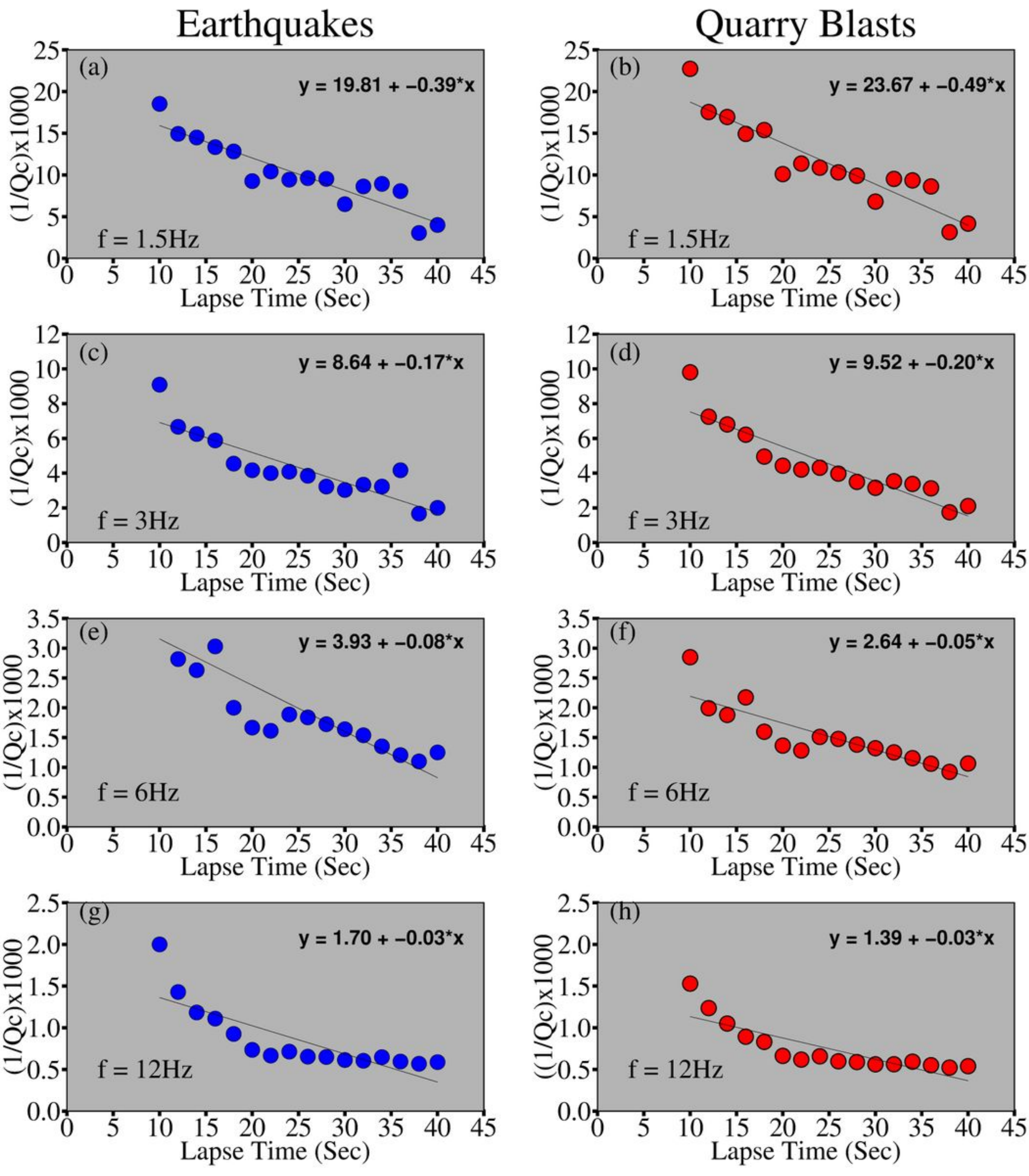

Figure 6

Qc inverse versus lapse time of earthquakes (a, c, e and g) and quarry blasts (b, d, f and h). The solid black line attributed to the best fit.

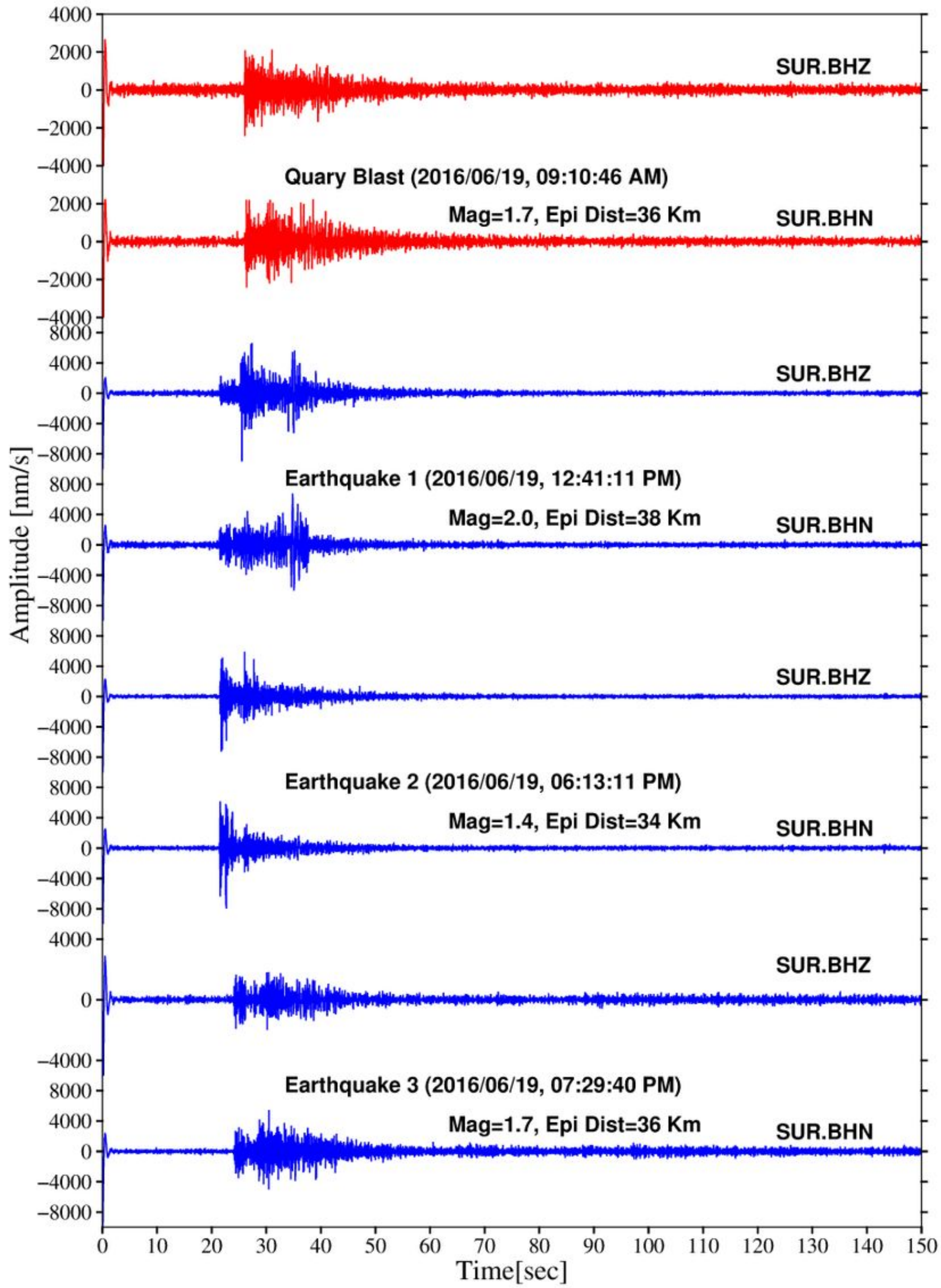

Figure 7

The vertical and horizontal component of quarry blast (red) and three induced microearthquakes (blue) on June 19, 2016 recorded at station SUR.

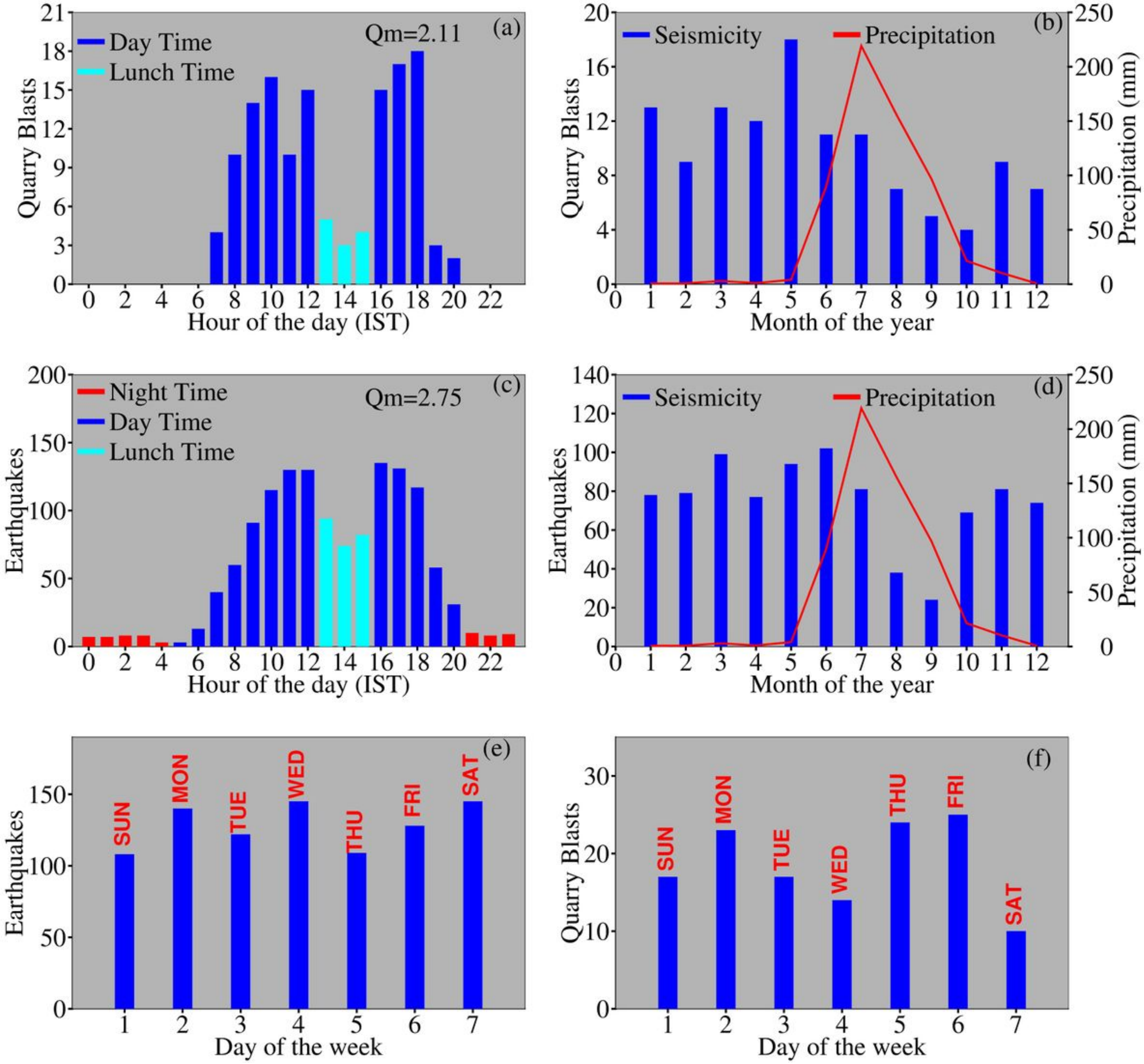

Figure 8

Histograms obtained after the discrimination.

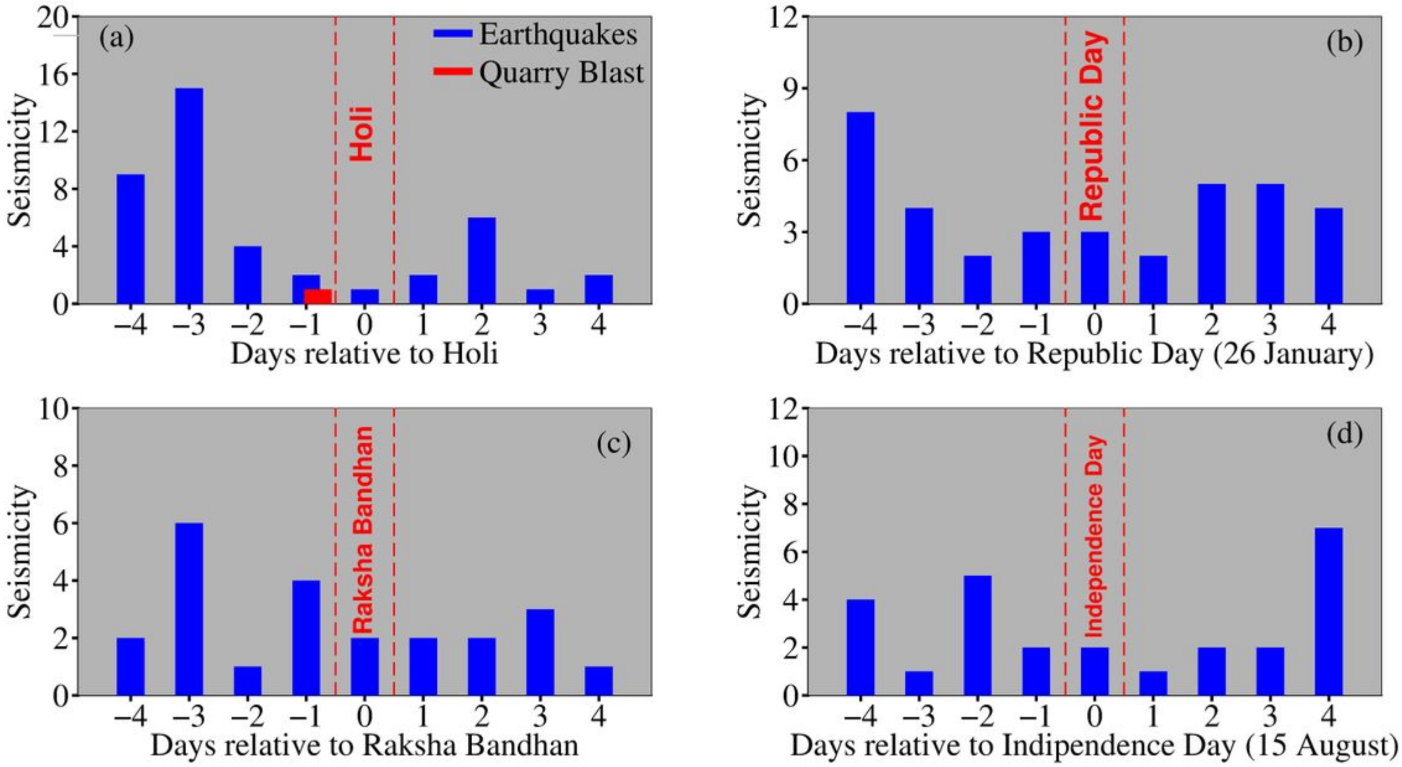

Figure 9

Distribution of seismic events four days before and after the different festivals in India between 2012 and 2016. We found no quarry blasts on these festivals.

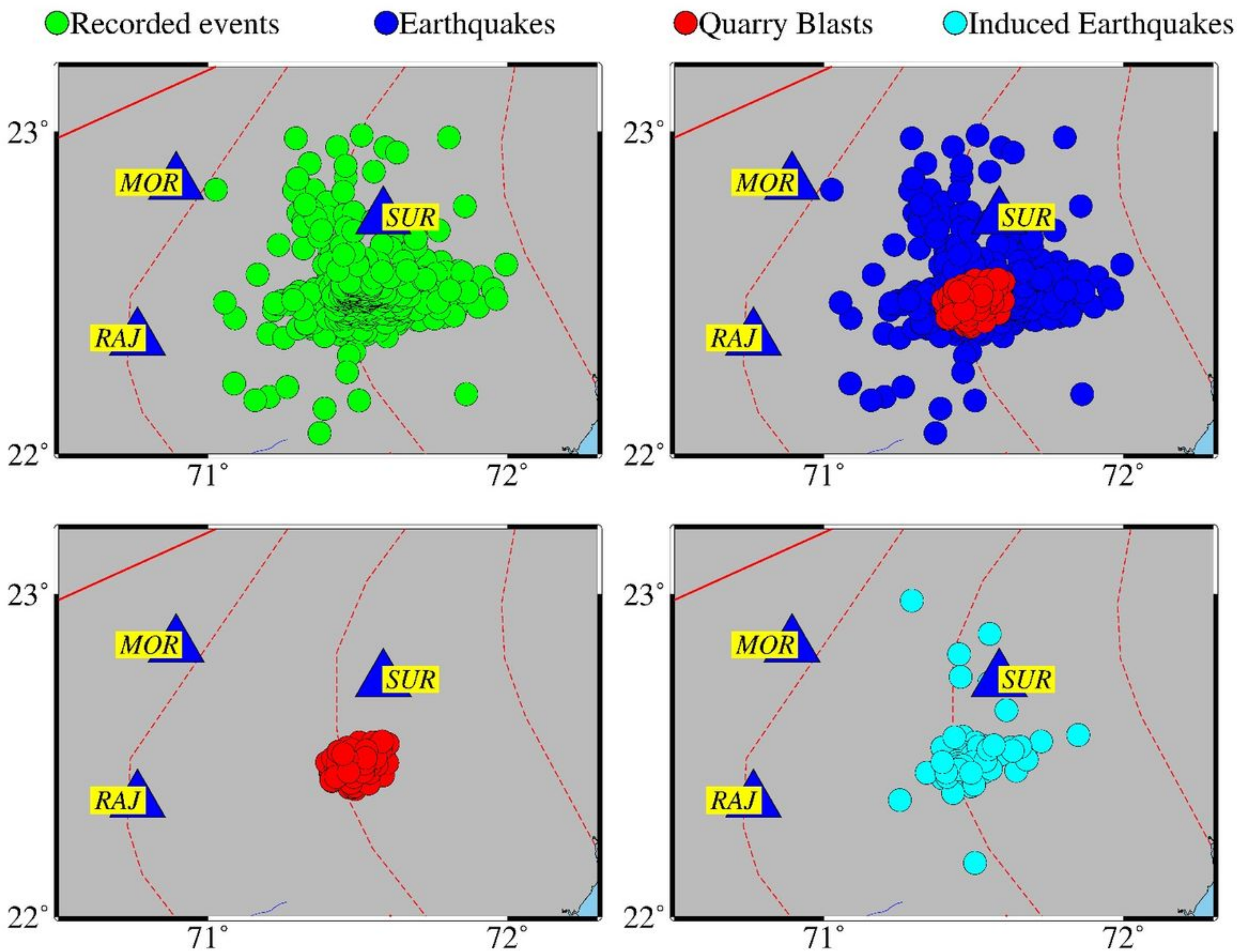

Figure 10

Location of quarry blasts and mining-induced earthquakes.

Supplementary Files

This is a list of supplementary files associated with this preprint. Click to download.

- graphicalabstractimage.png
- Suppliment.docx